APPLICATION OF FLEX-COMPRESSIVE PIEZOELECTRIC ENERGY HARVESTING CELL IN RAILWAY SYSTEM

Xianfeng Wang[1] and Zhifei Shi[1]

[1] School of Civil Engineering, Beijing Jiaotong University, Beijing 100044, P. R. China

Keywords: Piezoelectric, Energy harvesting, Flex-compressive, Large load, Railway

ABSTRACT

In the present study, an energy harvesting concept using flex-compressive energy harvesting cells embedded in the track structure is proposed. Based on beam theory and Winkler elastic foundation, a mechanical model of the track structure combined with energy harvesting devices embedded in the sleepers is established, and the theoretical performance of this energy harvesting system under moving loads is obtained. For a train with five cabins moving across the track with embedded flex-compressive energy harvesting cells, the power output of one energy harvesting cell is simulated. According to the numerical results, the weakened mode F-C PEHC has better energy harvesting performance compared with the enhanced mode one. While a train with 5 cabins runs over the energy harvester at the velocity of 40m/s, the power generation of enhanced mode F-C PEHC is 0.49W while that of the weakened mode F-C PEHC is 0.62W.

1 INTRODUCTION

Over the past few decades, China's railway system has made significant progress in both mileage and quality. During the operation of the railway system, monitoring the health status of the vehicles and the civil structures has become a critical issue. An effective way is to install wireless sensors on the vehicle bogies, rails, sleepers and wherever we need to monitor the health status such as velocity, acceleration, stress, etc. If we use traditional cables or batteries as the power sources of the wireless sensors, the alteration of the railway system and the replacement of the batteries will result in a huge cost. However, if we can harvest and utilize the mechanical energy hidden in the railway system as the power source of the wireless monitoring sensors building a self-sustained monitoring system, the promising benefits in both economy and security will be great. To achieve this vision, a reliable energy harvesting device with small size, simple structure and high conversion efficiency is required. As the piezoelectric material is with high power density and the ability to transform mechanical energy to electric power directly, the piezoelectric energy harvester just meet the above requirements.

The most commonly used piezoelectric energy harvesting structure is the cantilever beam or shaped cantilever beam. The cantilever structures work well for the ambient excitations such as base accelerations [1,2] or wind-induced vibrations [3,4]. For large mechanical excitations, cymbal type is the most commonly used architecture in the design of the piezoelectric energy harvesters. Piezoelectric stack is another architecture that is suitable for large pressure. Conventional cymbal type energy harvesters work in flex-tensional mode [5-7]. As we know, the tensile yield strength of piezoelectric ceramic is much lower than the compressive yield strength, which was found to be a limiting factor to the load capacity and life-time of the flex-tensional mode cymbal type energy harvesters. To utilize compressive stress in the piezoelectric component, flex-compressive piezoelectric energy harvesters are proposed by combining piezoelectric stacks with a cymbal type amplifier [8-10].

The flex-compressive piezoelectric energy harvesting cell proposed in our previous research is suitable for large load conditions acting as bearing structures. To utilize the large load provided by the train cabins, an energy harvesting concept using flex-compressive energy harvesting cells embedded in the track structure is proposed. In Section 2, the geometric details and mechanical equivalents of a track structure with flex-compressive energy harvesting cells embedded in the sleeper are described. In Section 3, the mechanical model of the track structure with embedded flex-compressive energy harvesting cells is established, and the theoretical performance of one flex-compressive energy harvesting cell under moving loads is obtained. In Section 4, for a train with five cabins moving across

the track with embedded flex-compressive energy harvesting cells, the power output of one energy harvesting cell is simulated and discussed. Section 5 concludes the study.

2 MECHANICAL EQUIVALENTS AND GEOMETRIC DETAILS

A flex-compressive mode piezoelectric energy harvesting cell (F-C PEHC) is an energy transducer with large load capacity assembled from two PZT stacks and four kinds of steel elements as shown in Figure 1. Since the F-C PEHC is mechanically assembled, there is no bonding layer, and all the components including the PZT stacks are replaceable. With different Element 1, both weakened mode (with large vertical stiffness and small equivalent piezoelectric constant) and enhanced mode (with small vertical stiffness and large equivalent piezoelectric constant) are achieved. According to our previous research, the vertical stiffness and equivalent piezoelectric constant of one F-C PEHC for both weakened and enhanced modes are presented in Table 1.

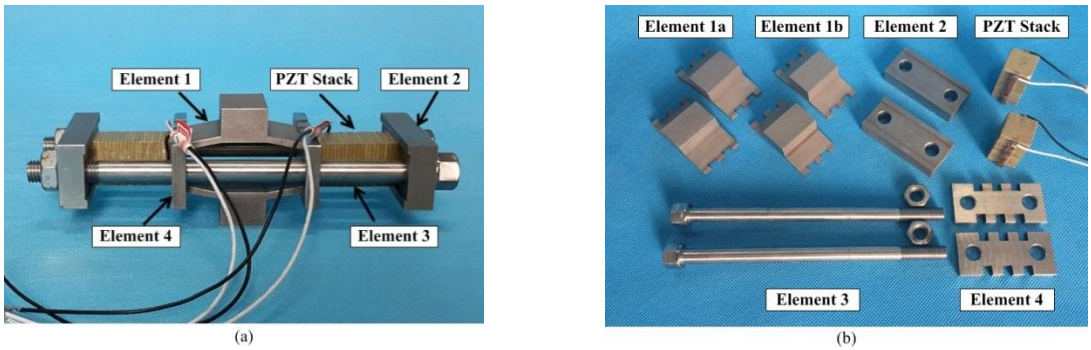

Figure 1: Configurations of the flex-compressive mode piezoelectric energy harvesting cell (F-C PEHC). (a) Prototype. (b) Individual Elements and the PZT stacks.

	k_p (MNm^{-1})	C_p^{eq} (nF)	d_{33}^{eq} (nC/N)
Weakened mode	17.20	353.6	19.92
Enhanced mode	6.71	353.6	41.28

Table 1: Equivalent parameters of one F-C PEHC.

To utilize the F-C PEHC in railway system, a schematic diagram of a typical track structure with F-C PEHCs embedded in the sleepers is proposed as shown in Figure 2. As illustrated in Figure 2, a typical track structure consists of the rail, the elastic pad the sleeper, the ballast bed and the foundation. The vertical stiffness ranges of each part of the track structure for one sleeper unit is indicated in Figure 2. In the following study, average values of upper and lower bounds are employed as presented in Table 2. The F-C PEHCs are installed between the rail and the sleeper paralleled to the elastic pad.

While the track structure with embedded F-C PEHCs is considered as a beam on a Winkler elastic foundation, the equivalent stiffness of the Winkler elastic foundation k could be expressed as

$$k = \frac{\left(k_p + k_e\right) k_b k_f}{\left[\left(k_p + k_e\right) k_b + \left(k_p + k_e\right) k_f + k_b k_f\right] d} \tag{1}$$

Where k_p is the vertical stiffness of one F-C PEHC, k_e is the vertical stiffness of the elastic pad, k_b is the stiffness of the ballast bed, k_f is the stiffness of the foundation, and d is the sleeper spacing.

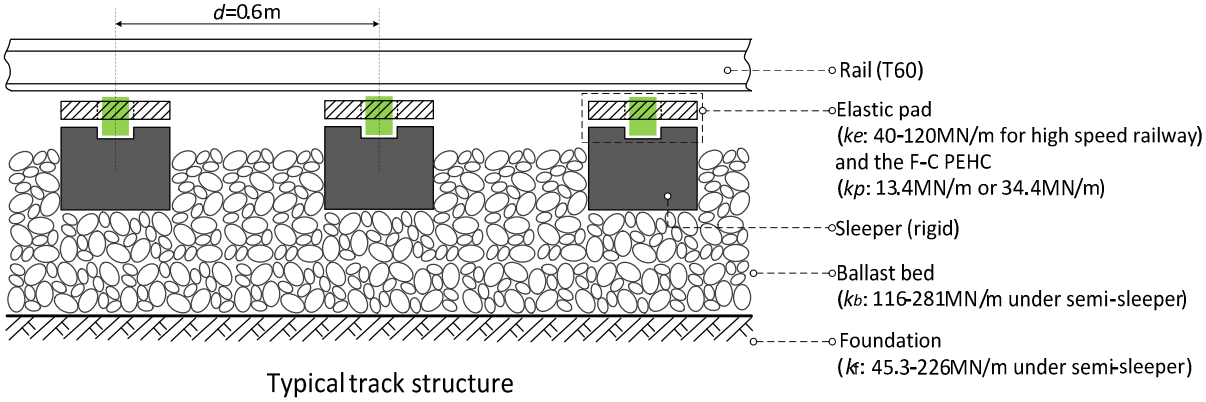

Figure 2: Schematic diagram of a typical track structure with F-C PEHC embedded in the sleepers.

Elastic pad stiffness k_e	80 MNm^{-1}
Ballast bed stiffness k_b	198.5 MNm^{-1}
Foundation stiffness k_f	135.7 MNm^{-1}
Rail bending stiffness EI	6.62 MNm^2
Rail mass ρ	60.64 kgm^{-1}
Sleeper spacing d	0.6m

Table 2: Mechanical parameters of the components in a typical track structure (one sleeper unit).

3 MECHANICAL MODEL

As shown in Figure 3, the present railway structure is simplified as a beam on a Winkler elastic foundation. The differential equation of motion for such structure is described as

$$EI\frac{\partial^4 w}{\partial x^4}+\rho\frac{\partial^2 w}{\partial t^2}+kw=\sum_{i=1}^{N}P_i\delta\left(x+l_i-vt\right) \tag{2}$$

Where $w=w(x, t)$ is the transverse deflection of the rail, E is Young modulus of the rail, I is the moment of inertia of the rail, EI is the Bending stiffness of the rail, ρ is the mass per unit length of the rail, P_i is the load of the ith pair of wheels, $-l_i$ is the initial space coordinate of the ith pair of wheels while t=0, δ is the Dirac delta function, and k is the equivalent stiffness of the Winkler foundation obtained in Section 2.

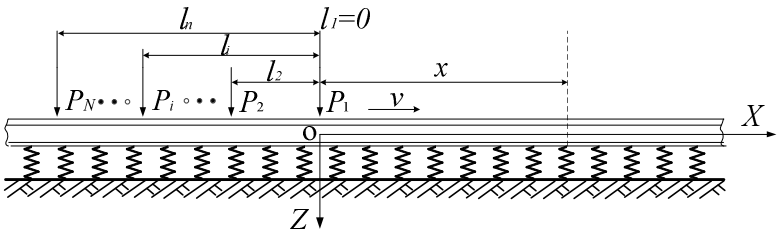

Figure 3: Mechanical model of track structure subjected to multiple moving loads.

Define $b^2=\frac{k}{EI}, a=\frac{\rho}{2EI}$, eq. (2) becomes

$$\frac{\partial^4 w}{\partial x^4}+2a\frac{\partial^2 w}{\partial t^2}+b^2 w=\sum_{i=1}^{N}\frac{P_i}{EI}\delta\left(x+l_i-vt\right) \tag{3}$$

And the critical velocity $v_{cr}^{\ 2} = b/a$ is defined. To avoid resonance, the train velocity should be smaller than v_{cr}. While $v < v_{cr}$, without the consideration of the damping influence, the steady-state solution of the transverse deflection of the rail can be derived as

$$w(x,t) = \sum_{i=1}^{N} w_i(x,t) \tag{4}$$

Where

$$w_i(x,t) = \begin{cases} \dfrac{P_i e^{-\alpha\xi_i}}{4EIb\alpha\beta}\left[\beta\cos\beta\xi_i + \alpha\sin\beta\xi_i\right], & \xi_i \geq 0 \\ \dfrac{P_i e^{\alpha\xi_i}}{4EIb\alpha\beta}\left[\beta\cos\beta\xi_i - \alpha\sin\beta\xi_i\right], & \xi_i < 0 \end{cases}$$

in which $\xi_i = x + l_i - vt$, $\alpha = \sqrt{\dfrac{b - av^2}{2}}$, $\beta = \sqrt{\dfrac{b + av^2}{2}}$.

For an F-C PEHC connected in parallel with a resistor *R*, the governing electromechanical equation could be obtained as

$$C_p^{eq}\dot{V}(t) + \frac{V(t)}{R} = d_{33}^{eq}F(t) \tag{5}$$

Where $V(t)$ is the voltage across the resistor, C_p^{eq} is the equivalent capacitance of one F-C PEHC, d_{33}^{eq} is the equivalent piezoelectric constant of one F-C PEHC, and $F(t)$ is the force applied on the F-C PEHC. Where $F(t) = \dfrac{k_p k w(L_0, t)}{k_p + k_e}$, in which L_0 is the coordinate of the studied F-C PEHC. With the initial condition $V(0) = 0$, the voltage across the resistor could be solved from eq. (5) as

$$V(t) = \sum_{i=1}^{N} V_i(t) \tag{6}$$

Where

$$V_i(t) = \frac{d_{33}^{eq}}{C_p^{eq}}\frac{k_p k w(L_0, t)}{k_p + k_e} - \frac{e^{-\frac{t}{RC_p^{eq}}}}{R\left(C_p^{eq}\right)^2}\left[\varphi_i(L_0, t) - \varphi_i(L_0, 0)\right] \tag{7}$$

In which

$$\varphi_i(x,t) = \frac{d_{33}^{eq}k_p k}{4EIb\alpha\beta\left(k_p + k_e\right)} \times \begin{cases} P_i e^{\frac{t}{RC_p^{eq}}} e^{-\alpha\xi_i}\left[\left(A_0\alpha + B_0\beta\right)\cos\beta\xi_i + \left(B_0\alpha - A_0\beta\right)\sin\beta\xi_i\right], & \xi_i \geq 0 \\ P_i e^{\frac{t}{RC_p^{eq}}} e^{\alpha\xi_i}\left[\left(-C_0\alpha - D_0\beta\right)\cos\beta\xi_i + \left(D_0\alpha - C_0\beta\right)\sin\beta\xi_i\right], & \xi_i < 0 \\ +P_i e^{\frac{x+l_i}{vRC_p^{eq}}} e^{\alpha\xi_i}\left(A_0\alpha + B_0\beta + C_0\alpha + D_0\beta\right) \end{cases} \tag{8}$$

The expressions of A_0, B_0, C_0, and D_0 are listed below:

$$A_0 = \frac{\beta v}{(\beta v)^2 + \alpha^2 \left(v + \frac{1}{\alpha R C_p^{eq}} \right)^2}, \quad B_0 = \frac{\alpha \left(v + \frac{1}{\alpha R C_p^{eq}} \right)}{(\beta v)^2 + \alpha^2 \left(v + \frac{1}{\alpha R C_p^{eq}} \right)^2}$$

$$C_0 = \frac{\beta v}{(\beta v)^2 + \alpha^2 \left(v - \frac{1}{\alpha R C_p^{eq}} \right)^2}, \quad D_0 = \frac{\alpha \left(v - \frac{1}{\alpha R C_p^{eq}} \right)}{(\beta v)^2 + \alpha^2 \left(v - \frac{1}{\alpha R C_p^{eq}} \right)^2}$$

Till now, the theoretical electrical output of an embedded F-C PEHC has been obtained.

4 NUMERICAL DISCUSSION

In this section, the energy harvesting performance of track structure combined with an embedded F-C PEHC is numerically discussed. A train with five cabins is employed as shown in Figure 3. The installation coordinate of the target F-C PEHC is taken as L_0=400d. The equivalent parameters of one F-C PEHC are presented in Table 1, and the mechanical parameters of the track structure are presented in Table 2.

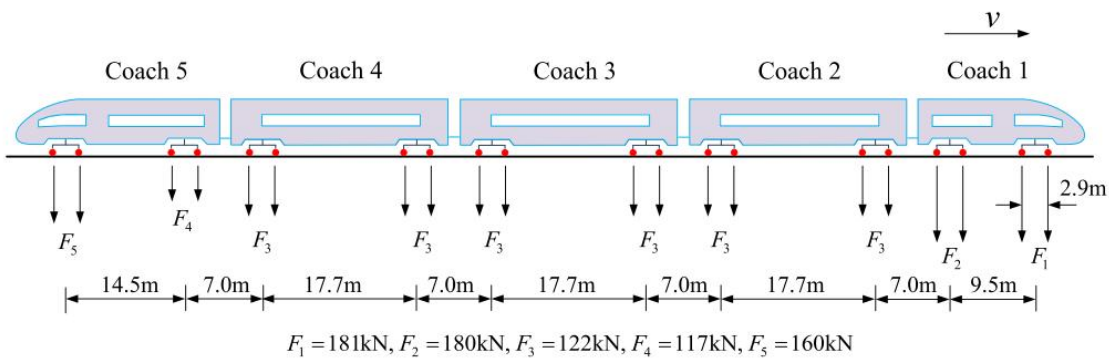

Figure 3: Geometric properties and the axle-loads of a train with 5 cabins.

Firstly, a weakened mode F-C PEHC is considered. While the train illustrated in Figure 3 runs over the track structure with an embedded weakened mode F-C PEHC, the time history of output voltage and power are presented in Figure 4. Note that the resistance R is taken as 180 kΩ. To evaluate the output voltage and power, the root mean square (RMS) is employed, which represent the valid value of the electrical output. In the following discussion, RMS is defined as $\sqrt{\frac{1}{T}\int_{T_1}^{T_2} f(t)^2}$. WhereT_1 and T_2 are the start and stop time of the effective signal, and T=T_1-T_2 is the effective time period. As we can see in Figure 4(a), for v=30m/s, the generated voltage and power are 230 V and 0.56 W, respectively. While the velocity increases to v=40m/s, the generated voltage and power increase to 236 V and 0.62 W, respectively as shown in Figure 4(b).

Secondly, an enhanced mode F-C PEHC is considered. As we can see in Figure 5(a), for v=30m/s, the generated voltage and power are 205 V and 0.45 W, respectively. While the velocity increases to v=40m/s, the generated voltage and power increase to 210 V and 0.49 W, respectively as shown in Figure 4(b).

Though the enhanced mode F-C PEHC has larger equivalent piezoelectric constant, the weakened mode F-C PEHC performs better in the numerical analysis. This is mainly because the F-C PEHC is parallel connected with the elastic pad. With large vertical stiffness, the weakened mode F-C PEHC bears more pressure compared with the enhanced mode.

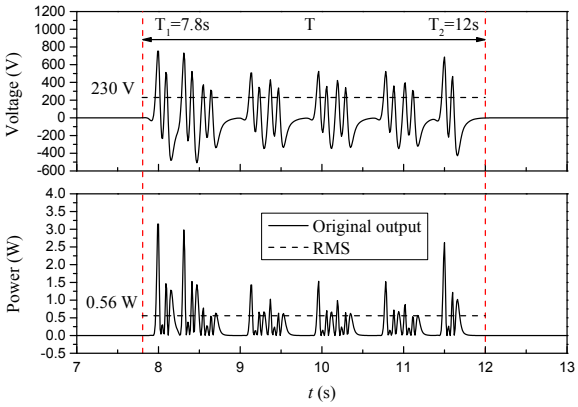

(a) v=30m/s

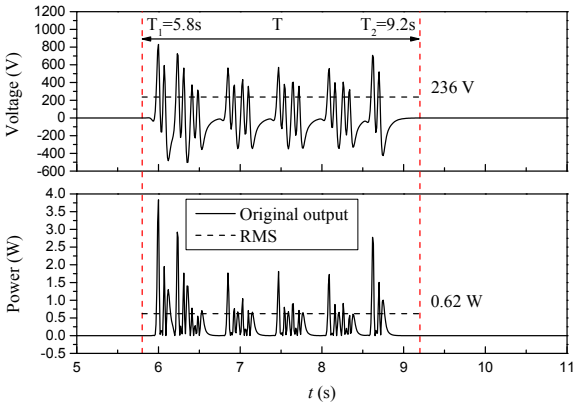

(b) v=40m/s

Figure 4: Time history of voltage and electric power (weakened mode). R=180kΩ. (a) v=30m/s. (b) v=40m/s.

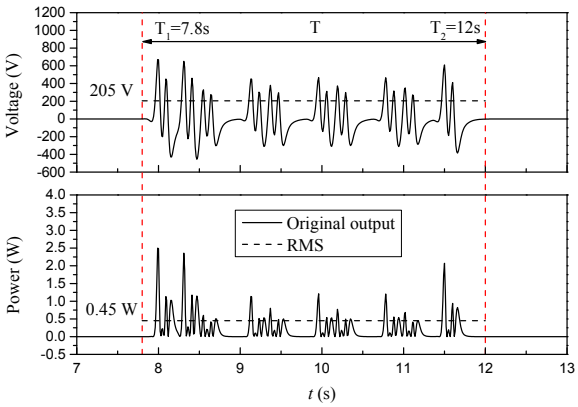

(a) v=30m/s

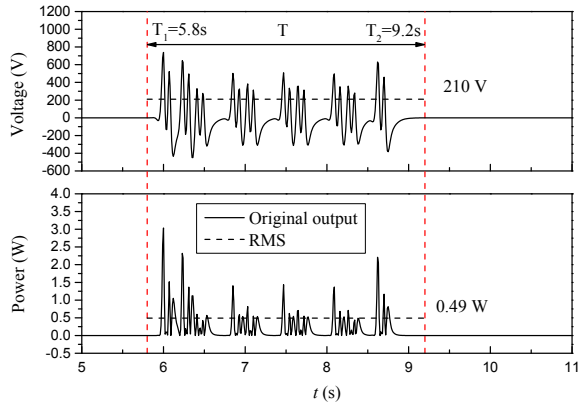

(b) v=40m/s

Figure 5: Time history of voltage and electric power (enhanced mode). R=180kΩ. (a) v=30m/s. (b) v=40m/s.

5 CONCLUSION

In the present study, a concept of railway energy harvesting using flex-compressive energy harvesting cells is proposed. Base on beam theory and Winkler elastic foundation, a mechanical model of the track structure combined with energy harvesting devices embedded in the sleepers is established, and the theoretical performance of this energy harvesting system under moving loads is obtained.

While a train with 5cabins runs over the F-C PEHC at the velocity of 40m/s, both weakened mode and enhanced mode F-C PEHC could generate watt level energy, i.e., 0.49W for the enhanced mode and 0.62W for the weakened mode. The present study demonstrated that the F-C PEHC has great potential in railway energy harvesting application.

ACKNOWLEDGEMENTS

This work is supported by the Fundamental Research Funds for the Central Universities (2016YJS104) and the National Natural Science Foundation of China (51472022 and 51522803).

REFERENCES

[1] H. A. Sodano, G. Park and D. J. Inman, Estimation of electric charge output for piezoelectric energy harvesting, *Strain*, **40**, 2004, pp. 49-58 (doi: 10.1111/j.1475-1305.2004.00120.x).

[2] Y. Liao and H. A. Sodano, Optimal placement of piezoelectric material on a cantilever beam for maximum piezoelectric damping and power harvesting efficiency, *Smart Materials and Structures*, **21**, 2012, pp. 105014 (doi: 10.1088/0964-1726/21/10/105014).

[3] A. Erturk, W. G. R. Vieira, C. De Marqui Jr, and D. J. Inman, On the energy harvesting potential of piezoaeroelastic systems, *Applied Physics Letters*, **96,** 2010, pp. 184103 (doi: 10.1063/1.3427405).

[4] D. Zhao and E. Ega, Energy harvesting from self-sustained aeroelastic limit cycle oscillations of rectangular wings, *Applied Physics Letters*, **105,** 2014, pp. 103903 (doi: 10.1063/1.4895457).

[5] H. W. Kim, A. Batra, S. Priya, K. Uchino, D. Markley, R. E. Newnham, and H. F. Hofmann, Energy harvesting using a piezoelectric "cymbal" transducer in dynamic environment, *Japanese Journal of Applied Physics*, **43**, 2004, pp. 6178-6183 (doi: 10.1143/JJAP.43.6178).

[6] H. W. Kim, S. Priya, K. Uchino, and R. E. Newnham, Piezoelectric energy harvesting under high pre-stressed cyclic vibrations, *Journal of Electroceramics*, **15,** 2005, pp. 27-34 (doi: 10.1007/s10832-005-0897-z).

[7] H. W. Kim, S. Priya and K. Uchino, Modeling of piezoelectric energy harvesting using cymbal transducers, *Japanese Journal of Applied Physics*, **45**, 2006, pp. 5836-5840 (doi: 10.1143/JJAP.45.5836).

[8] X. T. Li, M. S. Guo and S. X. Dong, A Flex-Compressive-Mode Piezoelectric Transducer for Mechanical Vibration/Strain Energy Harvesting, *IEEE Transactions on Ultrasonics,*

Ferroelectrics, and Frequency Control, **58**, 2011, pp. 698-703 (doi: 10.1109/TUFFC.2011.1862).

[9] X. F. Wang, Z. F. Shi, J. J. Wang, and H. J. Xiang, A stack-based flex-compressive piezoelectric energy harvesting cell for large quasi-static loads, *Smart Materials and Structures*, **25**, 2016, pp. 055005 (doi: 10.1088/0964-1726/25/5/055005).

[10] X. F. Wang and Z. F. Shi, Double piezoelectric energy harvesting cell: modeling and experimental verification, *Smart Materials and Structures*, **26**, 2017, pp. 065002. (doi: 10.1088/1361-665X/aa6cf9).